

Disappearance of a Stacking Fault in Hard-Sphere Crystals under Gravity

Atsushu MORI,^{*)} Yoshihisa SUZUKI, and Shigeki MATSUO

*Institute of Technology and Science, The University of Tokushima, Tokushima
770-8506, Japan*

At first, a review is given on a mechanism, which we have found recently by Monte Carlo (MC) simulations [A. Mori *et al.*, J. Chem. Phys. **124** (2006), 17450; Molec. Phys. **105** (2007), 1377], for the disappearance of an intrinsic stacking fault in a hard-sphere (HS) crystal under gravity. We have observed, in the case of fcc (001) stacking, that the intrinsic stacking fault running in an oblique direction was shrinking through the glide of the Shockley partial dislocation at the lower end of the stacking fault. To complement the shortcomings of those simulations, i.e., the systems have suffered from the periodic boundary condition (PBC) and the fcc (001) stacking have been realized by the stress from the small PBC box, we present a elastic strain energy consideration for the infinite system and a MC simulation result of hard spheres in a pyramidal pit under gravity. In particular, the geometry of the latter has already been tested experimentally [S. Matsuo *et al.*, Appl. Phys. Lett. **82** (2003), 4283]. That is, an advantage of the use of a pyramidal pit as a template as well as the feasibility of the mechanism we found is demonstrated.

§1. Introduction

It was in 1957 that existence of the crystalline phase in the hard-sphere (HS) system was found by Monte Carlo (MC) and molecular dynamics (MD) simulations;^{1),2)} the crystalline phase transition in the HS system is sometimes referred to as the Alder transition. It was surprised that the system comprised of merely hard-core repulsion exhibited the phase transition. An intuitive understanding of the Alder transition is given by decomposition of the entropy into those due to configurational variety of the centers of HSs and vibrational degree of freedom around their equilibrium positions. While in a disordered fluid phase the configurational entropy dominates, in the crystalline phase the vibrational one does. The HS system is in the fluid phase at the density lower than ϕ_f and in the crystalline phase of the face-centered cubic (fcc) structure at the density higher than ϕ_s , where the particle density is expressed in terms of the volume fraction of HSs $\phi \equiv \pi\sigma^3 N/6V$ with σ being the HS diameter, N the number of particles, and V the volume of the system. The crystal of ϕ_s coexists with the fluid of ϕ_f when the volume fraction of the total system lies between ϕ_f and ϕ_s . Hoover and Ree's values $\phi_f = 0.494$ and $\phi_s = 0.545$ ³⁾ determined by a MC method in 1968 have been revised in the last decade as $\phi_f = 0.491$ and $\phi_s = 0.542$ ⁴⁾ by a MD simulation study of direct two-phase coexistence (i.e., the crystal/fluid interface). We note that even the first MD simulation of the HS crystal/fluid interface was successful also in the last decade.⁵⁾

The present situation is a little different from that in the early years. In 1960-70's the existence of the colloidal crystals drew attention as an experimental realization

^{*)} E-mail: mori@opt.tokushima-u.ac.jp

of the Alder transition. The effective HS picture was proposed for charged colloids, which interacts through a screened Coulomb potential (though, the interparticle interaction is thus well described by a repulsive Yukawa form).⁶⁾ Nowadays, the HS system is not only an effective model of the colloids; poly(methylmethacrylate) (PMMA) particles with stabilizing polymers grafted on the particle surface⁷⁾ were developed as HS suspensions. PMMA particles are dispersed in a compounded hydrocarbon medium so that the HS nature with regard to the crystal-melt phase transition is exhibited.⁷⁾⁻¹¹⁾

There has been a background arisen, which should not be ignored. The colloidal crystals are potential materials used as photonic crystals.¹²⁾ To realize the photonic band, defects in the colloidal crystal should be reduced. To this end, many techniques have been developed. One of them is the colloidal epitaxy, in which a patterned substrate is used as a template to fix the stacking direction to be [001] in sedimentation of the colloidal particles.¹³⁾ Various patterns for the template have been examined, but this is not the present concern except for a single pyramidal pit.¹⁴⁾

A finding that has affected to the field of improving quality of the colloidal crystal is the effect of gravity on the crystallinity of the colloidal crystal; Zhu *et al.*¹⁵⁾ performed a colloidal crystallization on the Space Shuttle and concluded that while under microgravity the random hexagonal close pack (rhcp), under normal gravity the colloidal crystal formed by sedimentation is a rhcp/fcc mixture though the sometimes colloids freeze into a glassy state. Here, rhcp is the random stacking of hexagonal planes (fcc {111} or hcp (0001)); viewing along $\langle 111 \rangle$ the fcc is of ABCABC \cdots type and the hcp is of ABAB \cdots type while the rhcp corresponds to the random sequence. In other words, the stacking disorder can be reduced by gravity. We have, however, not reached to the final answer to the stacking sequence of colloidal crystals under gravity. Though the condition, i.e., the ratio of the gravitational length $l_g \equiv k_B T / mg$ to the HS diameter σ or the gravitational constant σ / l_g (we denote $g^* \equiv mg\sigma / k_B T$ hereafter) was different, Kegel and Dhont¹⁶⁾ reported the faulted twinned fcc under gravity. Here, $k_B T$ is the temperature multiplied by Boltzmann's constant and m the mass of the particle. We note that the temperature T should be defined from the thermal motion of the dispersing particles.

This paper focuses the mechanism of disappearance of the stacking disorder in the HS crystal under gravity. We have already demonstrated the disappearance of the stacking disorder in the HS crystal under gravity by MC simulations.¹⁷⁾ We have taken close looks where the shrinking of an intrinsic stacking fault was observed.¹⁸⁾ In § 2 we review those simulation results to bring their shortcomings into relief as well as to show what mechanism of disappearance of defect has been found. The objective of this paper is to provide some results to complement the shortcomings. The systems^{17), 18)} were highly stressed because of the smallness of the systems. We give some results of elastic energy calculation for the infinite system in § 3. The periodic boundary condition (PBC) applied in the simulations^{17), 18)} was one of the other artifacts. In § 4 we present results of MC simulation under a realizable boundary condition; HSs in a pyramidal pit¹⁴⁾ were simulated.

§2. Monte Carlo simulation under the Periodic Boundary Condition

In previous simulations¹⁷⁾ we presented results for two system sizes. One contained $N=1664$ particles and the other $N=3744$. In the former the fcc (001) stacking occurred while in the latter the stacking of the hexagonal layers were took place. We concentrated the former¹⁸⁾ because the defects disappearance was observed there. Though this side length equals $4a_0$, six particles lie along a side. Here, $a_0 = 1.57\sigma = (4\sigma^3/\rho_s)^{1/3}$ is the fcc lattice constant at the crystal/fluid coexistence of Hoover and Ree's value³⁾ with ρ denoting the particle density [$\phi \equiv (\pi/6)\rho\sigma^3$]. Six unit cells lay along a diagonal direction. In other words, [010] and [100] directed to the diagonal directions.¹⁹⁾ It indicates that the crystal at the bottom was at higher pressure than the crystal-fluid coexistence pressure [Hoover and Ree's value is $(P\sigma^3/k_B T)_{coex} = 11.75^3$) and Davidchack and Laird's one 11.55^4] in accordance with the mechanical balance equation

$$\partial P/\partial z = -mg\rho(z) \quad (2.1)$$

at the sedimentation equilibrium, where $\rho(z)$ is the particle density in coarse-scale at the altitude z . Also (2.1) implies that the lattice spacing along z direction varies as well as the unit cell is compressed in the vertical direction, i.e., the crystal is no longer of the cubic system, as confirmed.¹⁹⁾ The disappearance of stacking fault occurred under such artificially stressed condition. Such stress, however, plays a central role in defect reduction; as shall be described below the (001) stacking, in which the shrinking of the stacking fault occurred,¹⁸⁾ was induced thereby. Moreover, we, so far, make efforts on realizing the (001) growth, such as the colloidal epitaxy,¹³⁾ under a recognition that the stacking sequence for this growth is unique. Concentrating phenomena occurring under the (001) stacking, leaving the experimental realization of this stacking, is one of ways of elucidation.

In previous simulations^{17),18)} the gravitational constant g^* was changed step-wise to avoid the trapping of the system in the metastable state such as the polycrystalline state.²⁰⁾ We kept g^* at a certain value for 2×10^5 MC cycle (MCC) and then changed by $\Delta g = 0.1$, where one MCC is defined so as to include one position move per one particle on average. Transformation of a defective crystal into less-defective one in

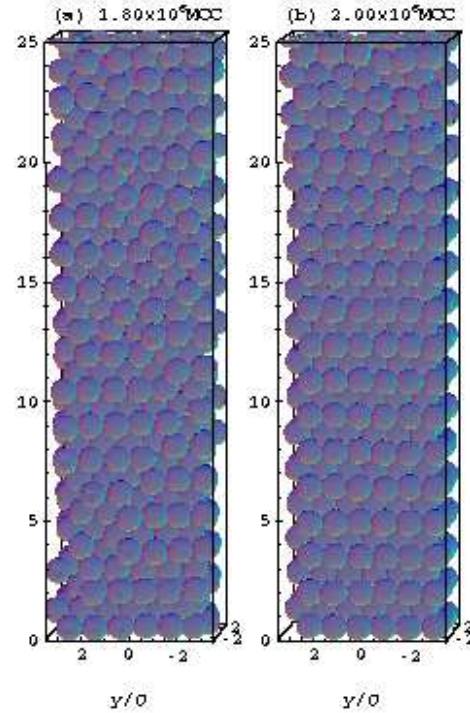


Fig. 1. Snapshots at the beginning (a) and the end of a MC simulation¹⁷⁾ with g^* being kept at 0.9.

the case of (001) stacking was observed around $g^* = 0.9$.¹⁷⁾ While g^* is kept at 0.9 for the (001) stacking case and we have found that shrinking of an intrinsic stacking fault is mediated by the glide of the Shockley partial dislocation terminating the bottom end of the stacking fault running in the oblique direction.¹⁸⁾ In Fig. 1 we see disappearance of stacking faults, which is running from the left-lower to the right-middle, [see, Ref. 18) for detail of the shrinking of the intrinsic stacking fault]. We stress that the advantage of the (001) stacking is not only the uniqueness of the stacking sequence but also the glide mechanism of the Shockley partial dislocation.

§3. Elastic Strain Energy Consideration

In this section we present the elastic energy calculation for a system including an intrinsic stacking fault running along [111]. The lower end of the stacking fault is terminated by the Shockley partial dislocation, such as shown in Ref. 18), and as is illustrated by Fig. 2. In this paper we incorporate the effect of the gravity as the buoyancy due to the particle deficiency accompanied by the dislocation core. The particle deficiency is one-third in Fig. 2. Though the crystal was indeed strained due to gravity¹⁹⁾ and, thus, the corresponding stress coupled with those due to the Shockley partial dislocation play a role promoting the shrinking of the intrinsic stacking fault, we can understand the shrinking of the intrinsic stacking fault without the cross term between them.

The Shockley partial dislocation terminating an intrinsic stacking fault running along [111], as shown in Fig. 2, is defined by the Burgers vector $\mathbf{b}^I = (1/6)[\bar{2}11]$ ($\equiv -\mathbf{a}_1/3 + \mathbf{a}_2/6 + \mathbf{a}_3/6$ with \mathbf{a}_1 , \mathbf{a}_2 , and \mathbf{a}_3 being the lattice vectors), which is shown by the arrow in Fig. 3. We understand the partial dislocation by decomposition of the perfect dislocation. In Fig. 3 $\mathbf{b} = (1/2)[\bar{1}10]$, the Burgers vector of a perfect dislocation, is decomposed as $\mathbf{b} = \mathbf{b}^I + \mathbf{b}^{II}$ with $\mathbf{b}^{II} = (1/6)[\bar{1}2\bar{1}]$ such as done in Ref. 21).

We calculate the elastic energy due to a dislocation running along unit vec-

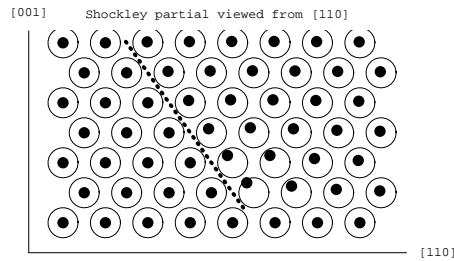


Fig. 2. Illustration of an intrinsic stacking fault. Particles in the distorted crystal are indicated by the dots and the regular lattice positions by open circles. Dotted line indicates the stacking fault. In this illustration particles outside the portion right of this line are not displaced for simplicity

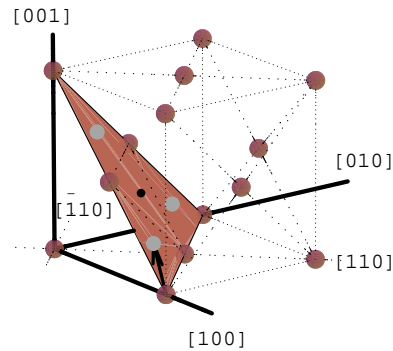


Fig. 3. The Burgers vector $\mathbf{b}^I = (1/6)[\bar{2}11]$ (arrow) and (111) plane (painted). The arrow connects a lattice position at, say, A and an adjacent one at, say, B.

tor $\boldsymbol{\xi}$ using a formula

$$W(R) = \frac{\mu b^2}{4\pi} \left(\cos^2 \theta + \frac{\sin^2 \theta}{1 - \nu} \right) \ln \left(\frac{\alpha R}{b} \right), \quad (3.1)$$

in the isotropic linear elastic theory,²¹⁾ where μ , ν , and θ are the shear modulus, the Poisson ratio, and the angle between the Burgers vector \mathbf{b} and $\boldsymbol{\xi}$, respectively, and b denoting $|\mathbf{b}|$. Here, α , which is several tenths, radius of the defines core region ($r_0 \equiv b/\alpha$). R is the dimension over which the elastic field expand, which we can usually identify with the radius of a crystallite or a grain. In the present case, where the stacking fault is running upward along $\langle 111 \rangle$ starting at the position of the Shockley partial dislocation, we simply regard R with the distance from the upper boundary to the Shockley partial dislocation. (Note that the dependence of the geometry of the boundary or the shape of the crystallite is innored.) Substituting \mathbf{b}^I for \mathbf{b} (i.e., $|\mathbf{b}^I| = a/\sqrt{6}$ with a being the fcc lattice constant) and $\boldsymbol{\xi} = (1/\sqrt{2})[\bar{1}10]$ (i.e., $\theta = \pi/6$), we have the elastic energy.

$$U_{el} = \frac{\mu a^2}{96\pi} \left(3 + \frac{1}{1 - \nu} \right) \ln \left(\frac{\sqrt{6}\alpha R}{a} \right). \quad (3.2)$$

Here and hereafter we consider the system of unit length thick perpendicular to Fig. 2. The core region is defined so that the linear elastic theory is valid outside that region. Borrowing the empirical result for metals;²¹⁾ U_{core} is proportional to μb^2 . Let us write $U_{core} = \beta \mu b^2$ with β being a certain constant of order less than unity. We have

$$U_{core} = \beta \mu a^2 / 6 \quad (3.3)$$

($\mathbf{b} = \mathbf{b}^I$) for the intrinsic stacking fault. Note that (3.3) is a constant with respect to R .

Here we should consider the stacking fault energy. This quantity as well as the elastic and core energies (rigorously, the free energies) is the entropic contribution — variety of vibrational mode distribution results in. Though the core energy has not been calculated, the shear modulus μ was calculated by a MC simulation²²⁾ and a density functional theory²³⁾ and the stacking faults energy γ_{sf} by a MC silulation.²⁴⁾ $\mu\sigma^3/k_B T$ for the HS crystal ranges between 50 and 100, depending on the particle number density ρ . This range of μ corresponds to $\rho\sigma^3 \cong 1.06 - 1.13$ ($a/\sigma \cong 1.55 - 1.52$) where the disappearance of the stacking disorder is observed in the MC simulations.^{17),18)} Stacking fault interfacial energy per unit area $\gamma_{sf}\sigma^2/k_B T$ is (at most) of order 10^{-4} at $\rho\sigma^3 = 1.10$. The difference of the order in μ and γ_{sf} has crucial important meaning; if the perfect dislocation decomposed into two partial dislocations connected by a stacking fault, the separation between two partial dislocations much longer than the order of the radius of a crystallite, which is typically a few or several hundreds of the lattice spacing. The total stacking fault energy is to be obtained by multiplying the length of the stacking fault, which is proportional to R as ζR ; the proportional constant ζ depends on the geometry of the boundary. Thus, we have $U_{sf} = \zeta \gamma_{sf} R$.

The gravitational energy is solely given by $U_g(R) - U_g(0) = m\rho a^2 R/3$, where we neglect the dependence of the particle density on the altitude. This approximate treatment is consistent with the treatment that we neglect the deformation according to (2.1). Here $U_g(R)$ the gravitational energy where the lower end of the stacking fault locates from the upper boundary of the crystallite; so $U_g(0)$ vanishes because the stacking fault goes out of the crystallite when $R = 0$. The sum of gravitational energy and the stacking fault energy is, thus, a linear function

$$U_{sf} + U_g = (\zeta\gamma_{sf} + m\rho a^2/3)R. \quad (3.4)$$

The total energy $U_{el} + U_{core} + U_{sf} + U_g$ constitutes a logarithmic term (3.2), a constant (3.3), and a linear term (3.4). The coefficient of the logarithmic term is positive and that of the linear term is apparently positive. It means that as R decrease, the energy decrease. We have shown by a elastic calculation that in the (001) stacking gravity yields a driving force that promotes the glide of the Shockley partial dislocation upward.

§4. Monte Carlo Simulation of Hard Spheres in a Pyramidal Pit

In the preceding two sections we consider two systems with artificial boundary conditions. In contrast, we treat in this section a realistic boundary condition; Matsuo *et al.*¹⁴⁾ used a pyramidal pit and groove to fix the stacking sequence. A pyramidal pit can be made by the anisotropic etching of the Si (001) surface (Fig. 4).

Contrary to the simulation under the PBC, the crystallinity is less sensitive to how the g^* was controled. This may be due to the wetting on the edges of the pyramidal pit (Fig. 5(a)). In Fig. 5 snapshots of MC simulations at $g^* = 0.1$ and 1.5 are shown; though $\Delta t = 2$ and 4×10^5 MCC where g^* was kept constant were also tested, results for $\Delta t = 1 \times 10^5$ MCC are shown. Figure 5(b) shows that despite the edge wetting the particles at the bottom was not crystallized. On the other hand, at the bottom of the pit crystallize the particles, particularly, in the fcc (001) stacking. In the pyramidal pit made of {111} faces, which can be made experimentally, the (001) stacking has been confirmed, as was already demonstrated experimentally.¹⁴⁾ Unfortunately, looking over the snapshots could not find the stacking faults and, thus, the glide mechanism of disappearance of the stacking fault was not observed. In our opinion, however, it is an indication of the robustness of this method against the stacking disorder; the epitaxial growth at the late stage start from the edges of the pit, on which the wetting occurs. In addition, the geometry of the boundary takes advantage; even if a crystallite mismatching its crystallographic

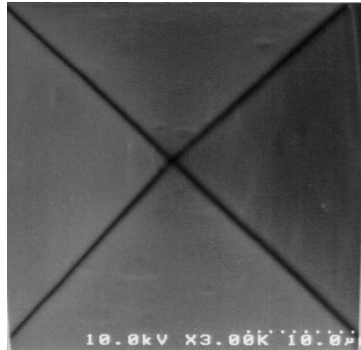


Fig. 4. A top view of a pyramidal pit made of four Si {111} face (scanning microscopy image).

orientation or lateral position with the crystal already formed nucleates at the bottom, the crystallite can slide along the wall. In other words, the simulation results does not rule out the glide mechanism of stacking fault, but pronounce its role.

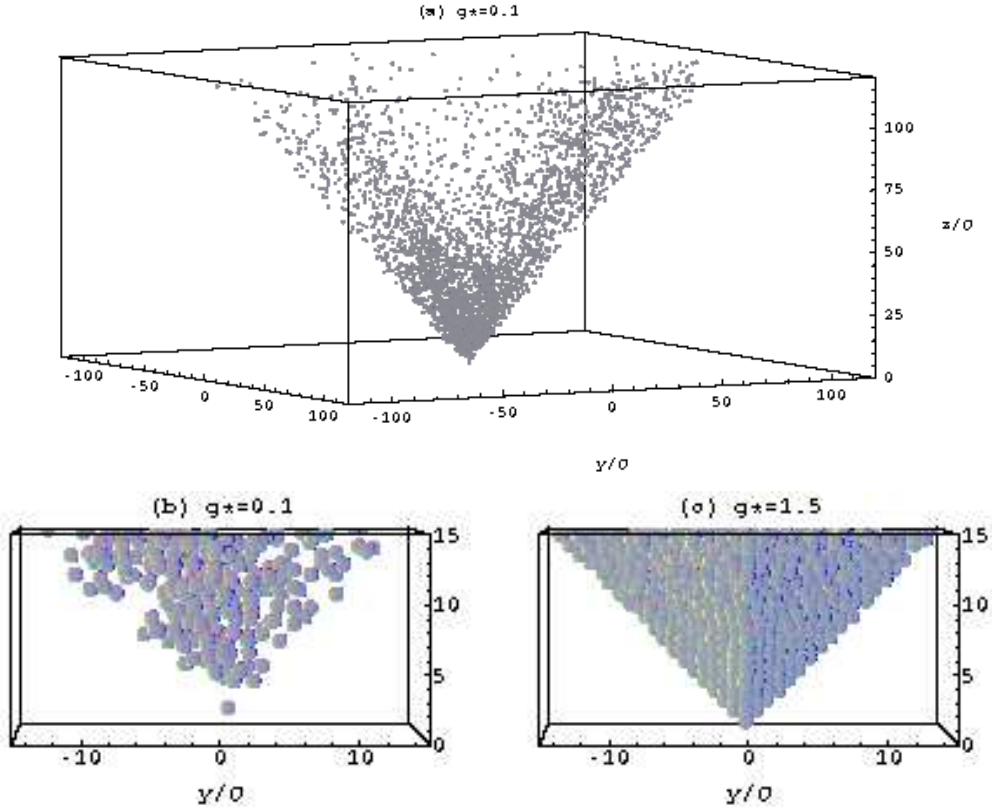


Fig. 5. Snapshots of MC simulation of HSs in a pyramidal pit. (a) An overview at $g^*=0.1$, where the edge wetting is seen, (b) a magnification of (a), and (c) a magnified snapshot at $g^*=1.5$, where crystalline order is observed.

§5. Discussions

Here we discuss about two simulations comparingly. Under the PBC the configuration is equivalent to the dislocation array of the same Burgers vector. On the other hand, owing to the concept of the mirror image, the pyramidal pit system is equivalent to the array of opposite charge. Whereas the former is less mobile, the dislocation in the latter does more easily disappear as one can understand by the pair annihilation of the opposite charge. The glide mechanism is implied likely because it is observed in the former configuration.

Cross term between gravity-induced elastic field and that due to the dislocation has not been treated in this paper. From (2.1) the particle density decrease as the altitude arises. It means that the buoyancy of the dislocation core is accelerated as the core goes up. An argument essentially the same is valid for strain energy to due

the dislocation.

§6. Concluding Remarks

We presented two simulation results and one theoretical calculation. All of them support the glide mechanism of disappearance of the stacking disorder in the hard-sphere crystal under gravity. We wish to emphasize that although this mechanism is not the final unique answer, it is likely.

In an elastic theoretical calculation we understand the glide mechanism without taking into account the cross term between gravity-induced elastic field and that due to the dislocation. That is, $\partial\sigma_{ij}/\partial x_i = 0$ with σ_{ij} being the stress tensor has been solved. Rigorous treatment is to solve $\partial\sigma_{ij}/\partial x_i + f_i = 0$ with f_i denoting the external force (gravitational force in the present case). This calculation is underway approximately using the result of Ref. 19).

References

- 1) W. W. Wood and J. D. Jacobson, *J. Chem. Phys.* **27** (1957), 1207.
- 2) B. J. Alder and T. E. Wainright, *J. Chem. Phys.* **27** (1957), 1208.
- 3) W. G. Hoover and F. H. Ree, *J. Chem. Phys.* **49** (1968), 3609.
- 4) R. L. Davidchack and B. B. Laird, *J. Chem. Phys.* **108** (1998), 3609.
- 5) A. Mori, R. Manabe, and K. Nishioka, *Phys. Rev. E* **51** (1995), R3831.
- 6) M. Wadach and M. Toda, *J. Phys. Soc. Jpn.* **32** (1972), 1147.
- 7) L. Antl, J. W. Goodwin, R. D. Hill, R. H. Ottweil, S. M. Owens, S. Parworth, and J. W. Waters, *Colloids Surf.* **17** (1986), 67.
- 8) P. N. Pusey and W. van Meges, *Nature* **230** (1986), 324.
- 9) S. E. Paulin and B. J. Ackerson, *Phys. Rev. Lett.* **64** (1990), 2663.
- 10) S. M. Underwood, J. R. Taylor, and W. van Meegen, *Langmuir* **10** (1994), 3550.
- 11) S. E. Phan, W. B. Russel, Z. Cheng, J. Zhu, P. M. Chaikin, J. H. Dunsмур, and R. H. Ottewil, *Phys. Rev. E* **54** (1996), 6633.
- 12) K. Sakoda, *Optical Properties of Photonic Crystal* (Springer-Verlag, Bargin, 2001).
- 13) A. van Blaaderen, R. Ruel, and P. Wiltzius, *Nature* **385** (1997), 312.
- 14) S. Matsuo, T. Fujine, K. Fukuda, S. Joudokazis, and H. Misawa, *Appl. Phys. Lett.* **82** (2003), 4283.
- 15) J. Zhu, M. Li, R. Rogers, W. Mayer, R. H. Ottiwil, STS-73 Space Shuttle Crew, W. B. Russel, and P. M. Chaikin, *Nature* **387** (1997), 1811.
- 16) W. K. Kegel and J. K. G. Dhont, *J. Chem. Phys.* **112** (2000), 3431.
- 17) A. Mori, S.-i. Yanagiya, Y. Suzuki, T. Sawada, and K. Ito, *J. Chem. Phys.* **124** (2006), 174507.
- 18) A. Mori, Y. Suzuki, S.-i. Yanagiya, T. Sawada, and K. Ito, *Molec. Phys.* **105** (2007), 1377.
- 19) A. Mori, S.-i. Yanagiya, Y. Suzuki, T. Sawada, and K. Ito, *Sci. Technol. Adv. Mater.* **7** (2006), 296.
- 20) S. i. Yanagiya, A. Mori, Y. Suzuki, Y. Miyoshi, M. Kasuga, T. Sawada, K. Ito, and T. Inoue, *Jpn. J. Appl. Phys. (Part 1)* **44** (2005), 5113.
- 21) J. P. Hirth and J. Lothe, *Theory of dislocation* (Krieger, Melabar, 1982).
- 22) D. Frenkel and A. J. C. Ladd, *Phys. Rev. Lett.* **59** (1987), 1169.
- 23) B. B. Laird, *J. Chem. Phys.* **97** (1992), 2699.
- 24) S. Pronk and D. Frenkel, *J. Chem. Phys.* **110** (1999), 4589.